8-2011

# The Effects of Retrogression and Reaging on Aluminum Alloy 2195

N. Ward

A. Tran

A. Abad

E. W. Lee

M. Hahn

*See next page for additional authors*

JMEPEG (2011) 20:1003–1014
DOI: 10.1007/s11665-010-9739-5

1059-9495/$19.00

# The Effects of Retrogression and Reaging on Aluminum Alloy 2195

*N. Ward, A. Tran, A. Abad, E.W. Lee, M. Hahn, E. Fordan, and O. Es-Said*

*(Submitted June 6, 2010)*

**A retrogression and reaging (RRA) treatment was performed on 2195 Al-Li Alloy. The exposure times were from 5 to 60 min, and the temperatures were from 200 to 250 °C. Samples that were exposed to a salt spray test had overall similar mechanical properties as compared to those that were not exposed. The percent elongation, however, was significantly deteriorated due to the salt spray exposure. The mechanical properties of the 2195 samples were compared to those of 2099 samples exposed to similar treatments in an earlier study.**

**Keywords** aluminum lithium alloys, retrogression and reaging, 2195 and 2099 alloys

## 1. Introduction

Retrogression and reaging (RRA) consists of heating peak-aged (T6) samples at high temperatures (retrogression) below the solvus line within a two-phase region for a short time and then reaging the materials at a low temperature and a long time (Ref 1, 2). RRA results in an optimum combination of strength and corrosion resistance (Ref 3). The resistance to corrosion of the retrogressed and reaged T-6 temper was due to coarsening of the grain boundary precipitates (Ref 4). The increase in volume fraction of the second-phase particles at the grain interior was responsible for the increase in strength (Ref 4-9).

Aluminum lithium alloys due to their low densities, tendency to super plastic forming, and high elastic modulii have been regarded as competitive structural materials for aerospace applications. Aluminum lithium alloy 2195 was developed to replace AA2219 which was being conventionally used to build the external tank of the USspace shuttles. It is a high strength, weldable alloy which provides a considerable mass reduction and increase in the pay load capability of the space shuttle (Ref 10-13).

The objective of this research was to study the effects of RRA treatments on a 2195 aluminum lithium alloy. In a previous study on 2099 Al-Li alloy (Ref 14), samples were subjected to a two-step T6-aging treatment that produced strength and ductility comparable to those of T8 temper samples, i.e., without stretching prior to aging. A similar two-step treatment (with different temperatures and times) were used in this study.

**N. Ward, A. Tran,** and **O. Es-Said**, Mechanical Engineering Department, Loyola Marymount University, Los Angeles, CA 90045-8145; **E.W. Lee**, Naval Air Systems Command, Naval Air Warfare, Patuxent River, MD 20670-1908; and **A. Abad, M. Hahn,** and **E. Fordan**, Northrop Grumman Aerospace Systems Air Combat Systems, El Segundo, CA 90045. Contact e-mail: oessaid@lmu.edu.

## 2. Experimental Procedure

The nominal composition of the alloy is shown in Table 1 (Ref 15). The 2195 plates were received with dimensions 0.91 m (3 ft) × 1.2 m (4 ft) × 0.013 m (0.5 in.) in the T3 temper. The samples were solution treated in a furnace at 450 °C for 1 h and then water quenched. Following quenching, the samples were naturally aged for 24 h, and then they were peak aged to the T6 temper at 165 °C for 24 h. This defined the starting T6 temper.

Samples in the T6 temper were retrogressed at 200, 220, 240, and 250 °C for 5 min, 10 min, 20 min, 40 min, and 1 h. Then they were reaged in one of two two-step aging processes. The first one was at 165 °C for 24 h followed by 177 °C for 16 h. The second was at 165 °C for 24 h followed by 177 °C for 24 h. These two-step processes are shown in Table 2.

Retrogression was conducted using a salt bath furnace and an oil bath furnace for 5-60 min and at 200-250 °C. Following retrogression, and prior to reaging, the samples were naturally aged for 24 h. All retrogression treatments were performed in an oil bath. Initially, a salt bath was used, however, the salt residue took longer time to remove before tensile testing. A Blue M Magni oil bath (Model: MW-1155C-2) was used for the oil bath, and a McEnglevan Speedy Melt Salt bath furnace (Model: P812) was used for the salt bath retrogression treatments.

After the reaging process, half of the samples were exposed to a salt fog test in accordance with ASTM B117 (Ref 16). Tensile specimens were machined in accordance with ASTM standard E-8 (Ref 17). Following the retrogression, the remaining oil or salt residues were removed by grinding with silicon carbide (grit 180) paper or by wiping any loose residue off. The tensile samples were rectangular plate specimens, with 203.2-mm (8.0 in.) total length, 50.8-mm (2.0 in.) gage length, 12.7-mm (0.5 in.) width, 57.15-mm (2.25 in.) length of reduced section, and 12.7-mm (0.5 in.) radius of fillet. The thickness of the samples was reduced to 6.35 mm (0.25 in.). The grips had 50.8-mm (2.0 in.) length and 19.05-mm (0.75 in.) width. Specimens were machined using standard milling machines and a CNC machine. Tensile tests were

**Table 1 Chemical composition of alloying elements in Al 2195**

| Chemical composition of Al 2195 | | | | | | | | |
|---|---|---|---|---|---|---|---|---|
| **Alloying element** | **Si** | **Fe** | **Cu** | **Mg** | **Mn** | **Ag** | **Li** | **Zr** |
| wt.% | 0.12 max | 0.15 max | 3.70-4.30 | 0.25-0.80 | 0.25 max | 0.25-0.60 | 0.80-1.20 | 0.08-0.16 |

**Table 2 Definition of reaging processes for Al 2195**

| Aging processes for Al 2195 | |
|---|---|
| **Aging process 1** | **Aging process 2** |
| 1. Heat at 165 °C for 24 h<br>2. Heat at 177 °C for 16 h | 1. Heat at 165 °C for 24 h<br>2. Heat at 177 °C for 24 h |

**Table 3 2195 T6 as-received properties (no salt spray exposure)**

| 2195 T6 as-received properties (no RRA) | | | |
|---|---|---|---|
| | **$\sigma_{ult}$, MPa (ksi)** | **$\sigma_{yield}$, MPa (ksi)** | **Percent elongation** |
| Sample 1 | 580 (84.2) | 513.0 (74.4) | Broke outside(a) |
| Sample 2 | 577.1 (83.7) | 496.4 (72.0) | 6.0 |
| As-received T6 (average) [average of samples 1 and 2] | 574.5 (83.9) | 504.7 (73.2) | 6.0 |
| As-received T8 standard (process 1) | 579.2 (84.0) | 537.8 (78.0) | 12.0 |

(a) The percent elongation was not calculated for samples which broke outside the gage length. The position of the fracture was slightly away from the gage, and the samples never failed in the radius or in the grip

**Table 4 2195 T6 as-received properties (salt spray exposure)**

| 2195 T6 as-received properties (no RRA) | | | |
|---|---|---|---|
| | **$\sigma_{ult}$, MPa (ksi)** | **$\sigma_{yield}$, MPa (ksi)** | **Percent elongation** |
| Sample 1 | 582.6 (84.5) | 498.5 (72.3) | 4.1 |
| Sample 2 | 580.5 (84.2) | 495.0 (71.8) | Broke outside(a) |
| As-received T6 (average) [average of samples 1 and 2] | 581.9 (84.4) | 497.1 (72.1) | 4.1 |
| As-received T8 standard (process 1) | 579.2 (84.0) | 537.8 (78.0) | 12.0 |

(a) The percent elongation was not calculated for samples which broke outside the gage length. The position of the fracture was slightly away from the gage, and the samples never failed in the radius or in the grip

performed using an Instron 4505 test frame at a constant cross head speed of 1.27 mm/min (0.05 in./min). All RRA samples were tested in duplicates. Only in the as-received condition,

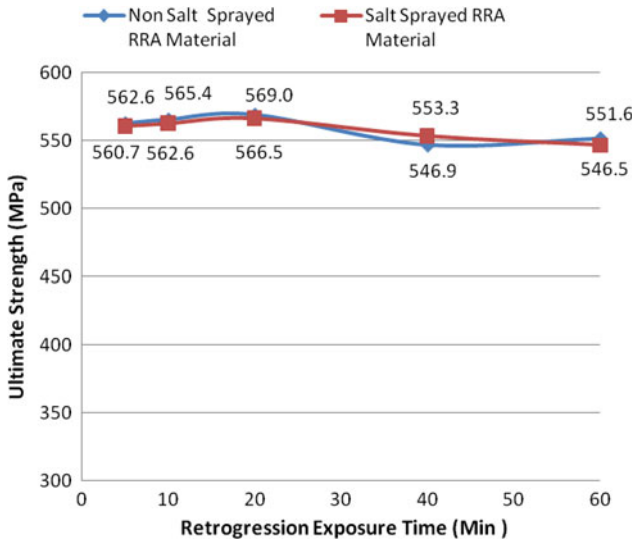


**Fig. 1** Ultimate strength vs. retrogression exposure time in RRA material with retrogression exposure temperature at 200 °C after reaging process 1

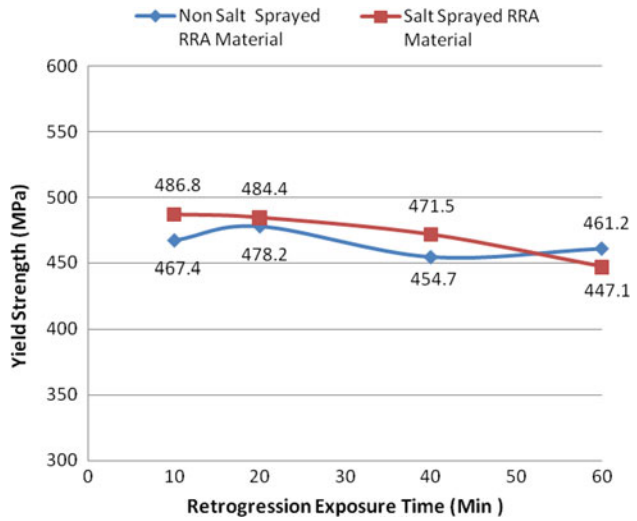


**Fig. 2** Yield strength vs. retrogression exposure time in RRA material with retrogression exposure temperature at 200 °C after reaging process 1

more than two samples were tested. Each data point was an average of the values obtained for two samples.

The fracture surface of the tensile samples were examined and characterized using a JEOL JSM-6400 Scanning Electron Microscope (SEM). Secondary electron imaging of the fracture surfaces was carried out at 15 kV, with about 30-50-mm working distance, the beam current was approximately 1 nanoamp.

## 3. Results and Discussion

The tensile properties of the T6 temper are shown in Table 3 and 4. The strength values were similar with and without salt spray exposure, but the percent elongation dropped by one-third of its original value from 6 to 4.1%.

The mechanical properties of the samples that were retrogressed at 200 °C versus the retrogression time (5, …, 60 min) for processes 1 and 2 are shown in Fig. 1, 2 and 3, 4, respectively. The ultimate strength values start from a high value at 5-10 min retrogression time (560-580 MPa) and decrease slightly (545-55 MPa) at 60 min (Fig. 1, 3). The samples which were exposed to the salt spray test had similar values to those that were not exposed. The yield strength values, Fig. 2 and 4, shows a similar trend to the ultimate strength values; however, the salt spray test samples had slightly higher values as compared to those who were not exposed in process 1 and lower values in process 2. The rate of drop in process 2 appears to be faster than that in process 1 (Fig. 2, 4).

The mechanical properties of the samples that were retrogressed at 250 °C versus the retrogression time, for processes 1 and 2 are shown in Fig. 5, 6 and 7, 8, respectively. The ultimate and yield strength values experience a drop during

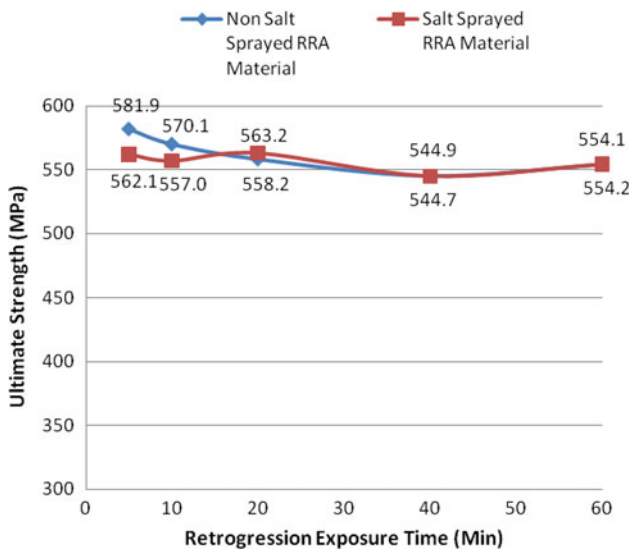


**Fig. 3** Ultimate strength vs. retrogression exposure time in RRA material with retrogression exposure temperature at 200 °C reaging process 2

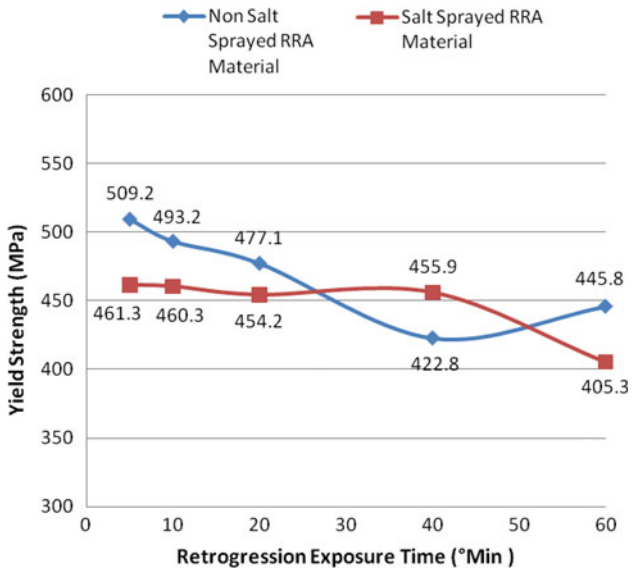


**Fig. 4** Yield strength vs. retrogression exposure time in RRA material with retrogression exposure temperature at 200 °C reaging process 2

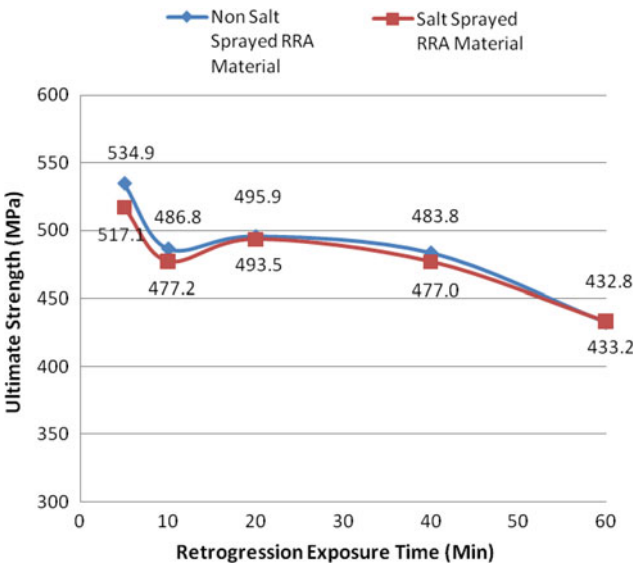


**Fig. 5** Ultimate strength vs. retrogression exposure time in RRA material with retrogression exposure temperature at 250 °C reaging process 1

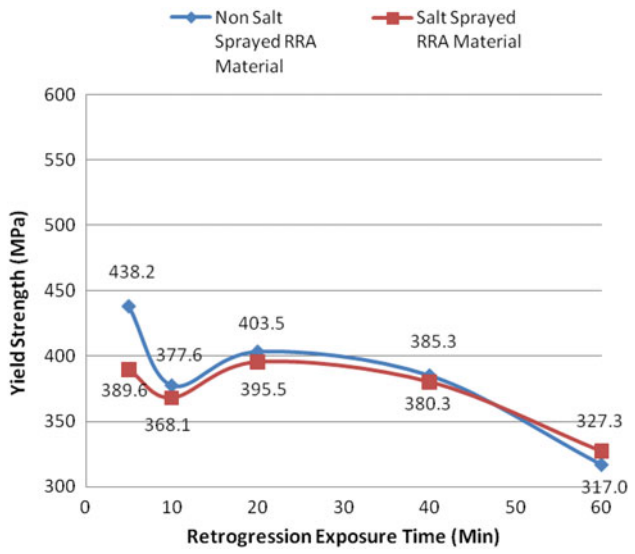


**Fig. 6** Yield strength vs. retrogression exposure time in RRA material with retrogression exposure temperature at 250 °C reaging process 1

retrogression time from 5 to 10 min, and then these values rise at around 10-20 min followed by a decreasing trend. The strength values at 250 °C were lower than those at 200 °C at all retrogression times. The rate of drop in the strength values was significantly higher at 250 °C as compared to those at 200 °C. The salt spray test samples had similar, or very slightly lower, mechanical property values as compared to those which were not exposed.

The mechanical properties of the samples that were retrogressed at 5 min versus the retrogression temperatures (200, …, 250 °C) for processes 1 and 2 are shown in Fig. 9, 10 and 11, 12, respectively. The ultimate strength values are similar in processes 1 and 2. These values drop gradually until 240 °C before they level off. The salt spray test samples had similar mechanical properties to those which were not exposed (Fig. 9, 11). The yield strength values, Fig. 10 and 12, showed a similar trend with a faster rate of drop.

The mechanical properties of the samples retrogressed at 20 min versus the retrogression temperature for processes 1 and 2 are shown in Fig. 13, 14 and 15, 16, respectively. The strength values show a gradual decline at temperatures ranging from 200 to 220 °C and then they leveled out. The salt spray samples had similar values to those which were not exposed. Both process 1 and 2 showed a similar trend.

The percent elongation of the samples retrogressed at 5 min versus the retrogression temperature for processes 1 and 2 is shown in Fig. 17 and 18. It is clear that the ductility of the non-salt-exposed samples are much better by a factor greater

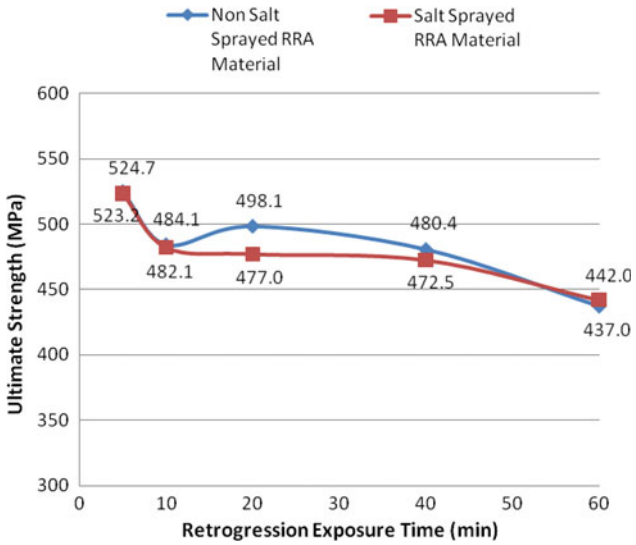


**Fig. 7** Ultimate strength vs. retrogression exposure time in RRA material with retrogression exposure temperature at 250 °C reaging process 2

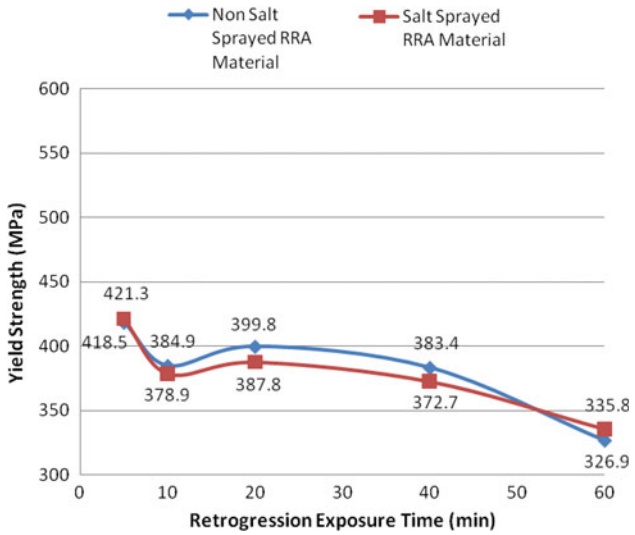


**Fig. 8** Yield strength vs. retrogression exposure time in RRA material with retrogression exposure temperature at 250 °C reaging process 2

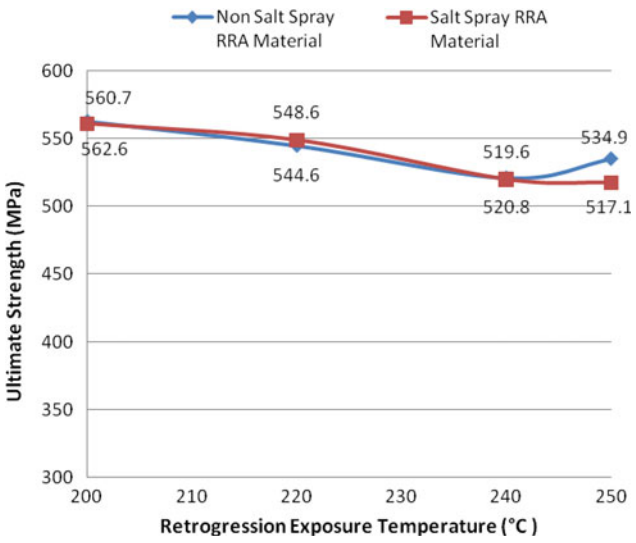


**Fig. 9** Ultimate strength vs. retrogression exposure temperature in RRA material with retrogression exposure time at 5 min after reaging process 1

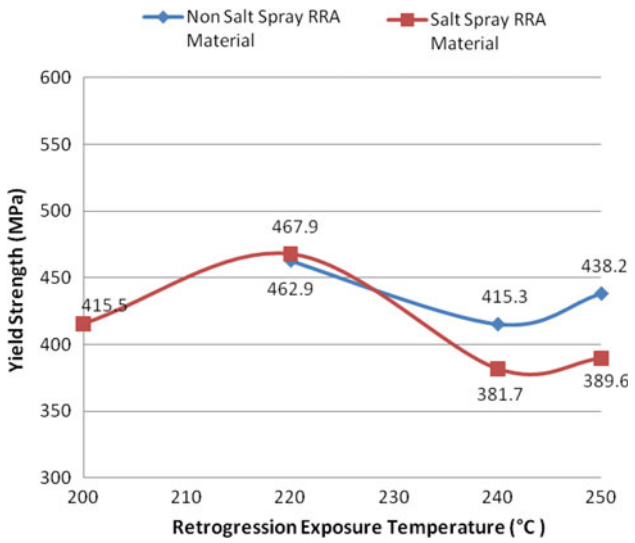


**Fig. 10** Yield strength vs. retrogression exposure temperature in RRA material with retrogression exposure time at 5 min after reaging process 1

than 2. The corrosive environment affected that salt-exposed samples and caused them to be brittle with a percent elongation of around 4%.

The ductility (percent elongation) was deteriorated by the salt spray exposure. Table 5 and 6 show the percent elongation for both non-salt spray- and salt spray-exposed samples for processes 1 and 2. The samples which were not exposed to the corrosive environment had higher values, around 2× those than that were exposed.

The microstructures of the fractured surfaces of the tensile samples (Fig. 19) were examined at different magnifications (100×, 1000×, and 2000×). The fractures were mostly brittle with intergranular mode in all samples.

The ultimate and yield strength values gradually dropped in accordance with the study of other researchers (Ref 3-9) as the retrogression time and/or temperature increased. The best retrogression time/temperature that maintained the high strength values of the salt spray-exposed samples was the combination of 200 °C/5-60 min for both processes 1 and 2. This also is in accordance with earlier study on the 7xxx series aluminum alloys (Ref 7-9, 18).

The ultimate strength values (Fig. 1, 3, 5, 7, 9, 11, 13, 15) at all retrogression times and temperatures indicated that the salt-exposed samples had the same strength values as those that were not exposed. The yield strength values (Fig. 2, 4, 6, 8, 10, 12, 14, 16) showed a similar trend, however, the salt-exposed

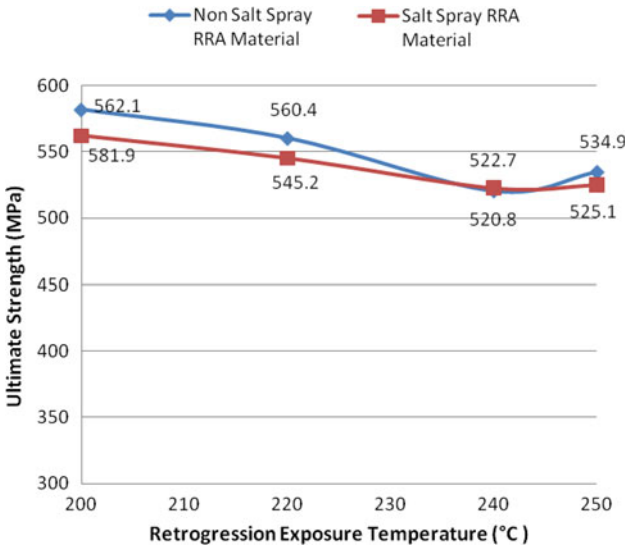


**Fig. 11** Ultimate strength vs. retrogression exposure temperature in RRA material with retrogression exposure time at 5 min after reaging process 2

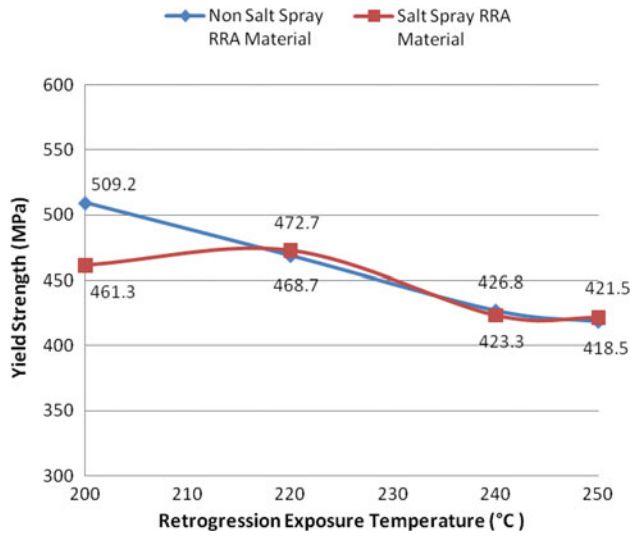


**Fig. 12** Yield strength vs. retrogression exposure temperature in RRA material with retrogression exposure time at 5 min after reaging process 2

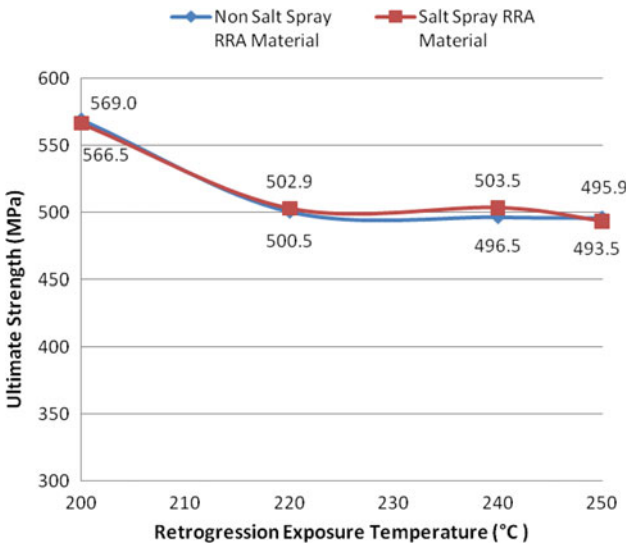


**Fig. 13** Ultimate strength vs. retrogression exposure temperature in RRA material with retrogression exposure time at 20 min after reaging process 1

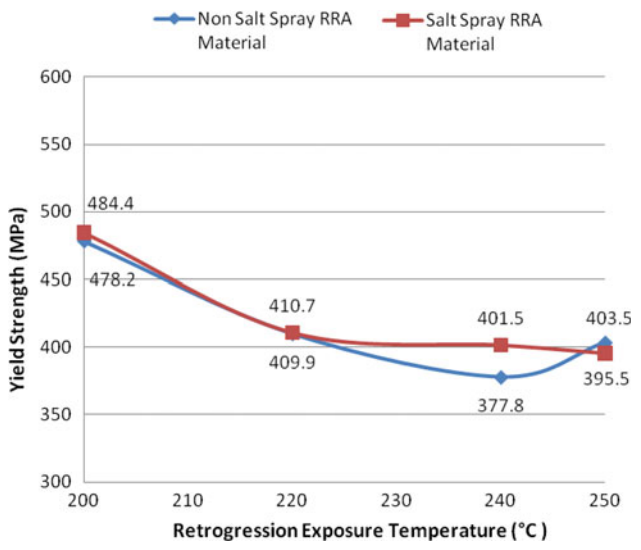


**Fig. 14** Yield strength vs. retrogression exposure temperature in RRA material with retrogression exposure time at 20 min after reaging process 1

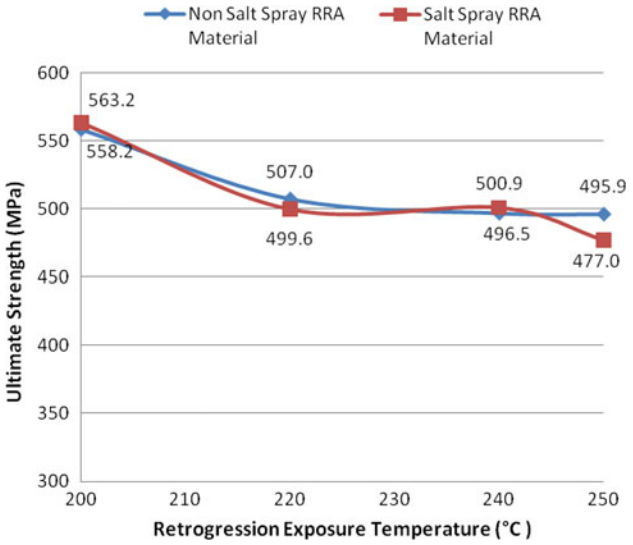


**Fig. 15** Ultimate strength vs. retrogression exposure temperature in RRA material with retrogression exposure time at 20 min after reaging process 2

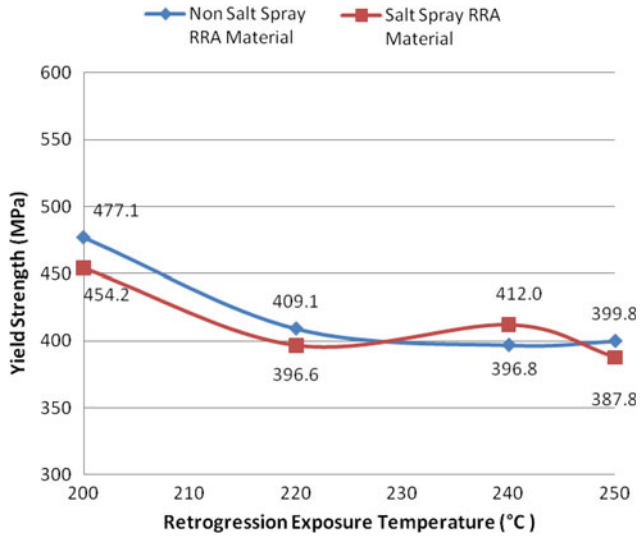


**Fig. 16** Yield strength vs. retrogression exposure temperature in RRA material with retrogression exposure time at 20 min after reaging process 2

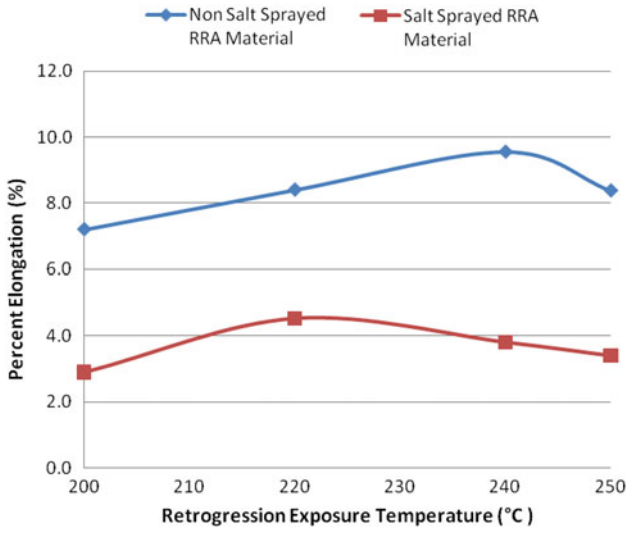


**Fig. 17** Percent elongation vs. retrogression exposure temperature in RRA material with retrogression exposure time at 5 min after reaging process 1

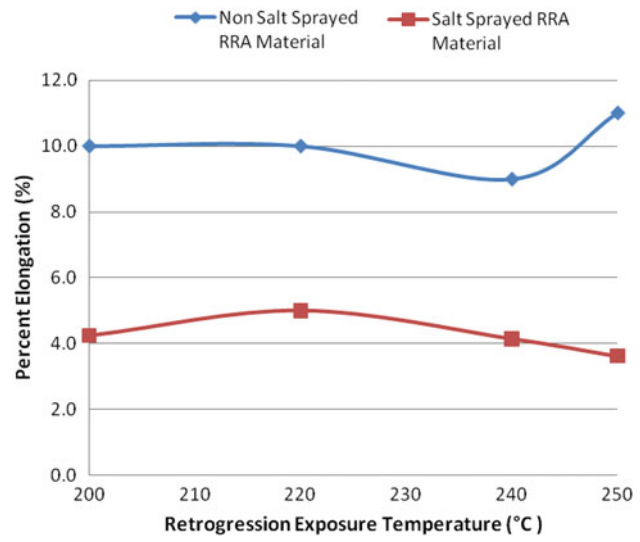


**Fig. 18** Percent elongation vs. retrogression exposure temperature in RRA material with retrogression exposure time at 5 min after reaging process 2

**Table 5 Percent elongation data for non-salt-exposed samples**

| Non-salt spray | | | | |
|---|---|---|---|---|
| Percent elongation (process 1\|process 2) | | | | |
| | Temp., °C | | | |
| Time, min | 200 | 220 | 240 | 250 |
| 5 | 7.2\|6.5 | 6.6\|8.2 | 9.6\|9 | 7.2\|11 |
| 10 | 7.0\|6.5 | 6.6\|8.2 | 9.1\|7.3 | 6.9\|6.3 |
| 20 | 7.1\|6.5 | 8.2\|9.3 | 8.1\|5.5 | 6.7\|8.5 |
| 40 | 7.1\|7.8 | 4.6\|8.2 | 6.4\|6.9 | 7.2\|6.9 |
| 60 | 10.5\|5.1 | 6.9\|7.0 | 7.9\|7.5 | 8.0\|7.9 |

**Table 6 Percent elongation data for non-salt-sprayed samples**

| Salt spray | | | | |
|---|---|---|---|---|
| Percent elongation (process 1\|process 2) | | | | |
| | Temp., °C | | | |
| Time, min | 200 | 220 | 240 | 250 |
| 5 | 2.9\|4.3 | 4.5\|5.0 | 3.8\|4.2 | 3.4\|3.6 |
| 10 | 4.0\|5.3 | 6.4\|4.4 | 5.0\|5.8 | 3.3\|5.1 |
| 20 | 2.9\|3.8 | 4.5\|4.7 | 4.5\|4.5 | 4.3\|4.9 |
| 40 | 2.8\|5.7 | 5.5\|4.4 | 4.1\|4.4 | 4.6\|5.4 |
| 60 | 2.0\|4.7 | 3.6\|3.8 | 5.3\|5.5 | 5.8\|6.6 |

samples sometimes had slightly lower or slightly higher values as compared to those which were not exposed. The yield strength values of the salt-exposed samples had a large scatter for almost all conditions. That is to say, for a certain retrogression temperature and time, samples will show the same ultimate strength values, but the yield strength values may differ by around 21-69 MPa (3-10 ksi).

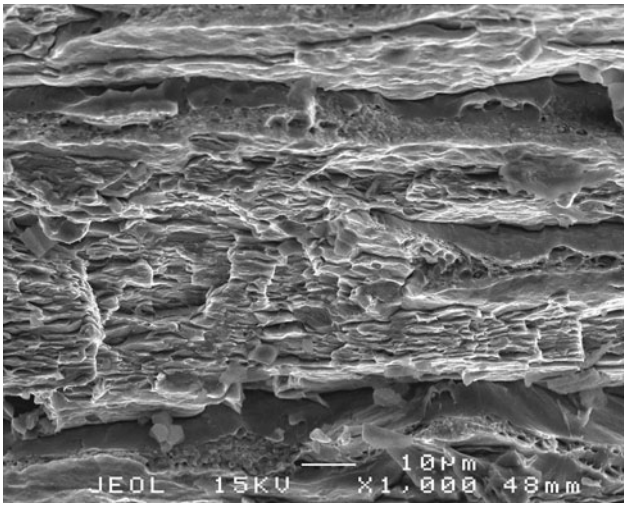


**Fig. 19** SEM micrograph 2195 alloy at 1000× magnification (Al 2195 process 1, 250 °C for 20 min)

## 4. Comparison Between the 2099 and 2195 Aluminum Lithium Alloys

In a recent study by the same authors (Ref 19), a similar RRA treatment, with different reaging temperatures and times was performed on a 2099 T-8 aluminum-lithium alloy. The 200 °C retrogression temperature for all times (5, …, 60 min) yielded the best RRA process in terms of maintaining the strength values in the salt spray tests similar to the results obtained in this study on the 2195 alloy. In the 2099 alloy (Ref 19), however, the samples exposed to the corrosive environment (salt spray test, ASTM B117) had consistently higher strength values compared to those which were not exposed. This result is not the same for the 2195 alloy. In this study, the 2195 alloy samples exposed to the salt fog test had around the same strength values as compared to the samples that were not exposed to the salt spray test. The reason for this difference in response to the salt spray test is not clear. The consistent higher strength values of the salt-exposed samples as compared to the samples that were not exposed to the corrosive environment in the 2099 alloy could not be explained by an aging effect corresponding to the ASTM B117 test. In this test, the samples were exposed to a temperature maintained at 35 °C for 168 h (1 week). This temperature is not warm enough to cause an aging effect. It might be related to the difference in chemical composition of both alloys, Table 7 (Ref 20).

The 2195 alloy has higher contents in Si, Fe, Cu, Mg, and Zr, and lower contents in Zn and in Li. In addition, 2195 has Ag (0.25-0.6 wt.%) which is missing in the 2099. Ag is added as a

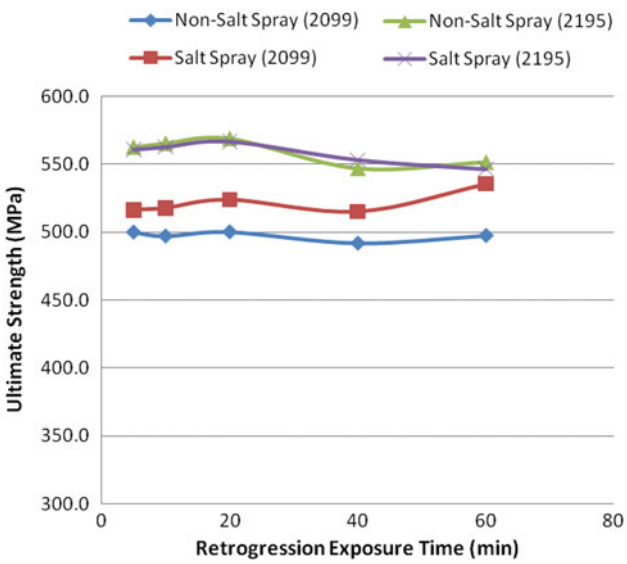


**Fig. 20** Ultimate strength vs. retrogression exposure time, 200 °C, process 1 for both 2099 and 2195

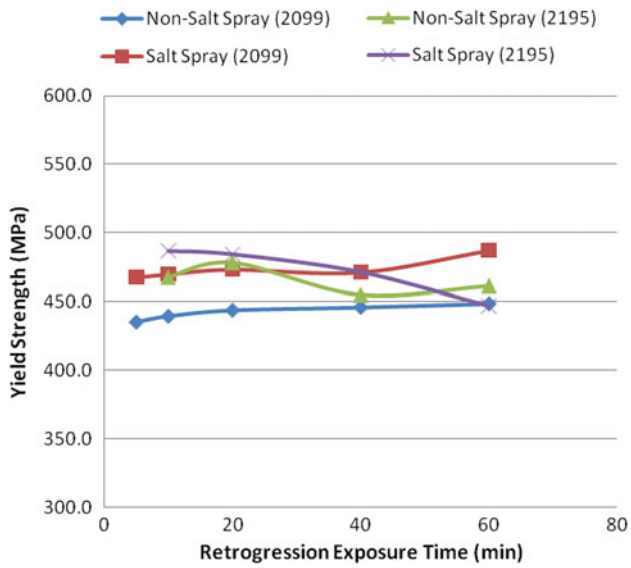


**Fig. 21** Yield strength vs. retrogression exposure time, 200 °C, process 1 for both 2099 and 2195

**Table 7 Weight percent (wt.%) of different solutes in 2099 and 2195 aluminum lithium alloys (Ref 16)**

| No. | Si | Fe | Cu | Mn | Mg | Zn | Ti | Ag | Li | Zr | Al |
|---|---|---|---|---|---|---|---|---|---|---|---|
| 2099 | 0.05 | 0.07 | 2.4-3.0 | 0.10-0.50 | 0.10-0.50 | 0.40-1.0 | 0.1 | … | 1.6-2.0 | 0.05-0.12 | Rem. |
| 2195 | 0.12 | 0.15 | 3.7-4.3 | 0.25 | 0.25-0.8 | 0.25 | 0.1 | 0.25-0.6 | 0.8-1.2 | 0.08-0.16 | Rem. |

nucleating agent to enhance the precipitation of the main strengthening phase $T_1$ (Ref 21). Basically the 2195 alloy is an Al-Cu-Li-Mg-Ag alloy, and the 2099 is an Al-Cu-Li-Mg alloy. Cu is added to form $T_1$ ($Al_2CuLi$) and θ′ type ($Al_2Cu$) strengthening phases and $T_2$ ($Al_6CuLi_3$) which increases toughness (Ref 21). Zn is added to improve corrosion resistance, maybe that's why 2099 showed better retention of ductility. Mg is added for strengthening. Mn is added to homogenize dislocations slip to improve fracture toughness and fatigue properties and Zr is added to inhibit recrystallization (Ref 22). Probably a solute present in the 2099 alloy interacted with the sodium chloride to cause this slightly higher strength in the salt-exposed samples. The mechanical properties of the 2099 (Ref 19) and the 2195 aluminum-lithium alloys are plotted at 200 °C retrogression temperature versus retrogression time (5, …, 60 min) in Fig. 20-23. The ultimate strength values of the 2195 alloy are higher than those of the 2099 (Fig. 20, 22). The yield strength values of the 2195 alloy gradually decrease a function of the retrogression time. That drop is not observed in the 2099 alloy. It appears that the salt-exposed 2099 retains its strength values (Fig. 21, 23). The mechanical properties at 250 °C retrogression temperature is plotted versus retrogression time in Fig. 24-27. The same trend is observed similar to retrogression at 200 °C, that is to say the 2195 alloy has higher strength values but these values drop faster than those of the 2099 alloy. All the strength values of

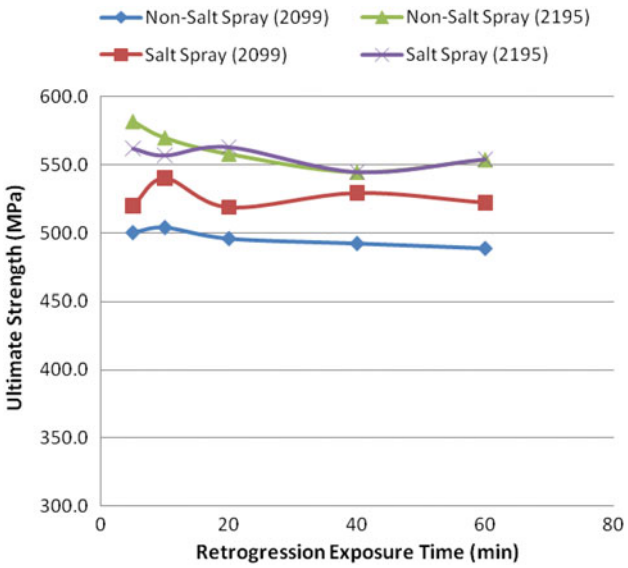


**Fig. 22** Ultimate strength vs. retrogression exposure time, 200 °C, process 2 for both 2099 and 2195

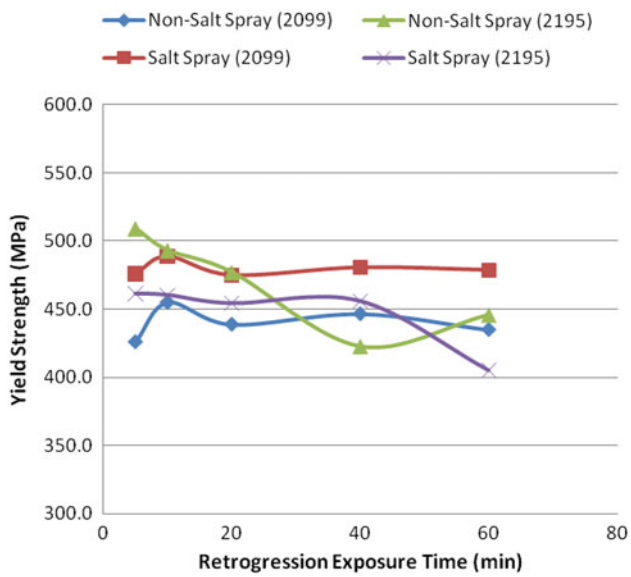


**Fig. 23** Yield strength vs. retrogression exposure time, 200 °C, process 2 for both 2099 and 2195

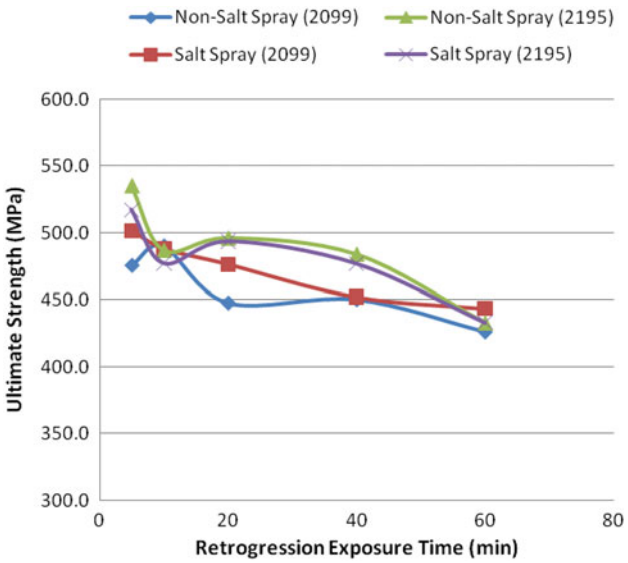


**Fig. 24** Ultimate strength vs. retrogression exposure time, 250 °C, process 1 for both 2099 and 2195

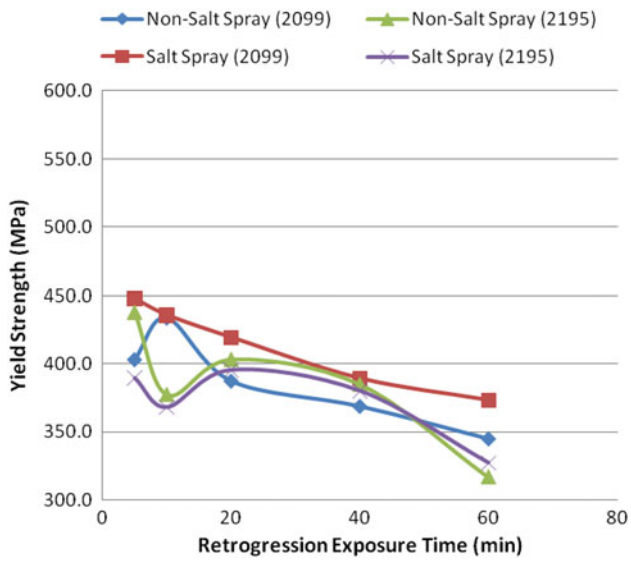


**Fig. 25** Yield strength vs. retrogression exposure time, 250 °C, process 1 for both 2099 and 2195

both alloys drop significantly as the retrogression time increases. However, the yield strength values of the salt spray 2099 alloy appears to be higher than all the other alloys.

The mechanical properties retrogressed for 10 min for both alloys for process 1 are plotted versus the retrogression temperature (200, …, 250 °C) in Fig. 28 and 29. The ultimate strength values are higher for the 2195 alloy however they coincide with the values of the 2099 alloy at 240 °C (Fig. 28). The drop in yield strength values of the 2195 alloy was faster than the drop in the 2099 alloy to the extent that they were significantly lower than those of the 2099 alloy at 240 °C (Fig. 29). A slight increase in the strength values of all alloys occur between 240 and 250 °C probably due to solute reversion (Ref 23). The mechanical properties retrogressed for 60 min retrogression temperature for both alloys for process 1 are plotted in Fig. 30 and 31. The ultimate strength values again for the 2195 alloy are higher but they coincide with the values of the 2099 alloy at 240-250 °C (Fig. 32). The yield strength values drop significantly and rapidly for both alloys equally. This was expected due to the long exposure time (60 min) at all retrogression temperatures.

The microstructures of the fracture tensile bars clearly indicated a mixed fracture mode for the 2099 alloy (Ref 19). A mixture of equiaxed dimples and intergranular fracture was observed in all the samples tested. The microstructures of the 2195 on the other hand clearly showed mostly an intergranular

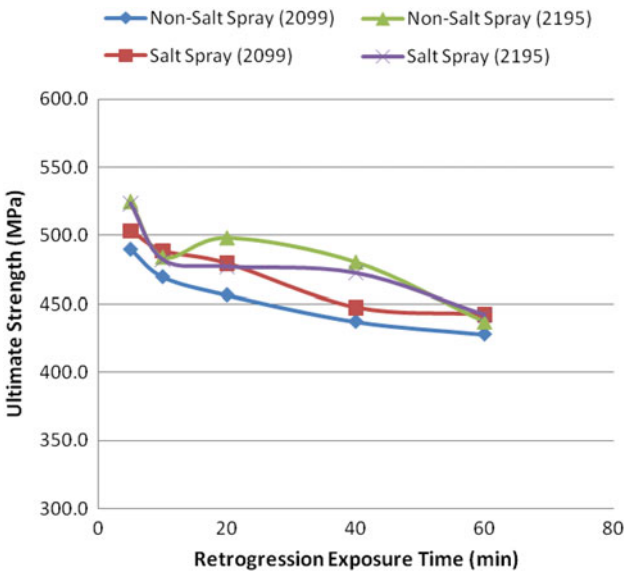


**Fig. 26** Ultimate strength vs. retrogression exposure time, 250 °C, process 2 for both 2099 and 2195

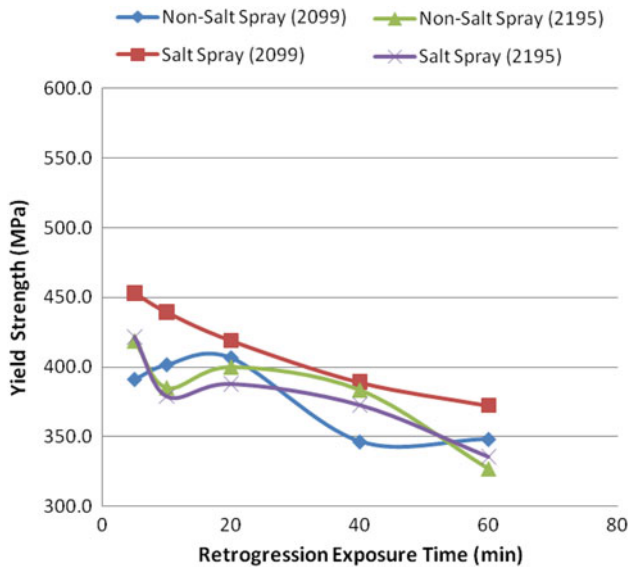


**Fig. 27** Yield strength vs. retrogression exposure time, 250 °C, process 2 for both 2099 and 2195

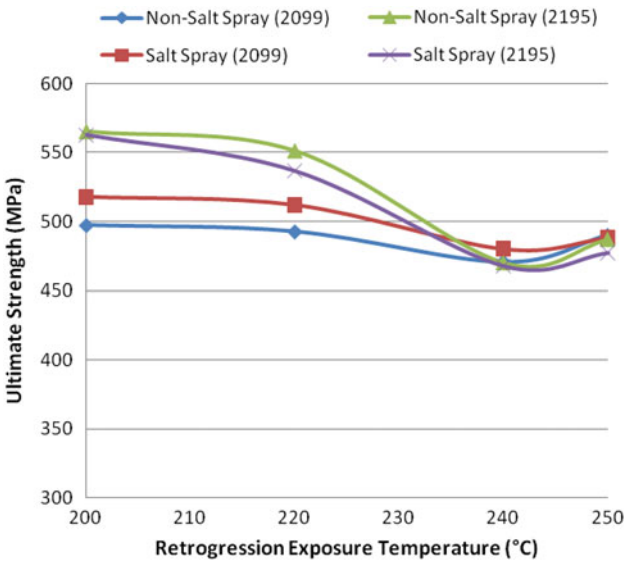


**Fig. 28** Ultimate strength vs. retrogression exposure temperature, 10 min, process 1 for both 2099 and 2195

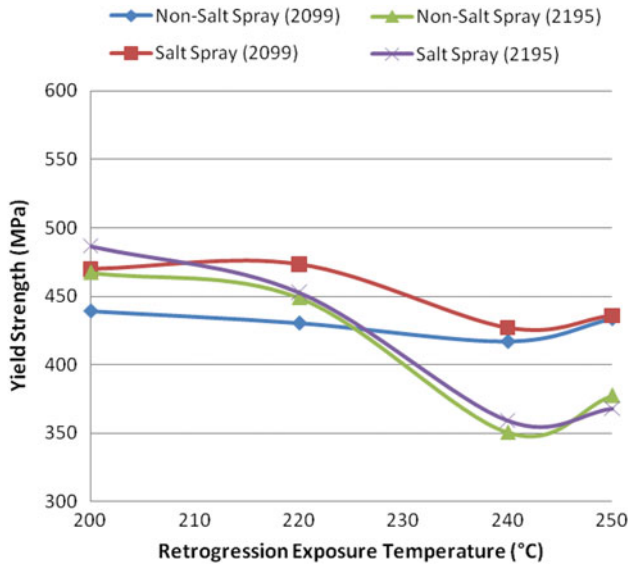


**Fig. 29** Yield strength vs. retrogression exposure temperature, 10 min, process 1 for both 2099 and 2195

fracture mode (Fig. 32a, b). This is in accordance with the ductility data of both alloys. The average percent elongation of all tensile samples for both alloys in both processes are shown in Table 8 and 9. The range of values for the 2099 non-salt sprayed was between 7.5 and 16% while those for the 2195 were between 4.6 and 10.5%. The range of values for the 2099 salt-sprayed samples was between 8.5 and 11% while that for the 2195 was between 3.6 and 6.6%.

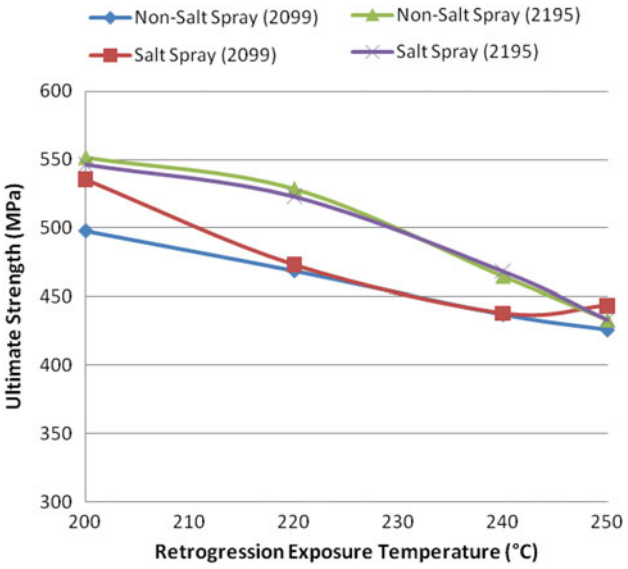


**Fig. 30** Ultimate strength vs. retrogression exposure temperature, 60 min, process 1 for both 2099 and 2195

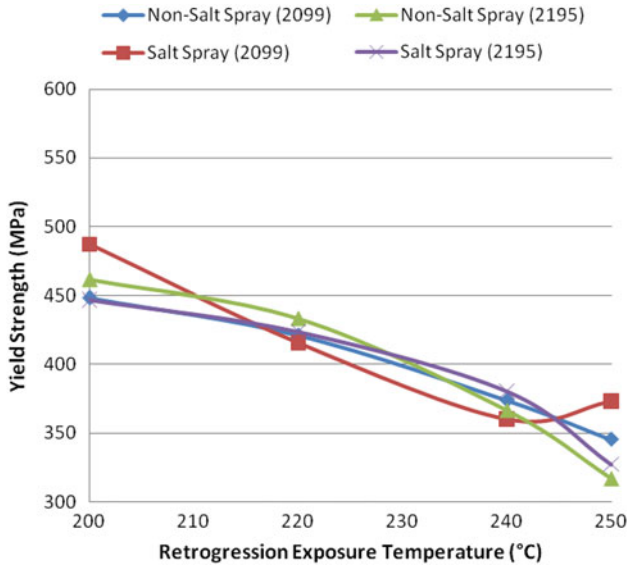


**Fig. 31** Yield strength vs. retrogression exposure temperature, 60 min, process 1 for both 2099 and 2195

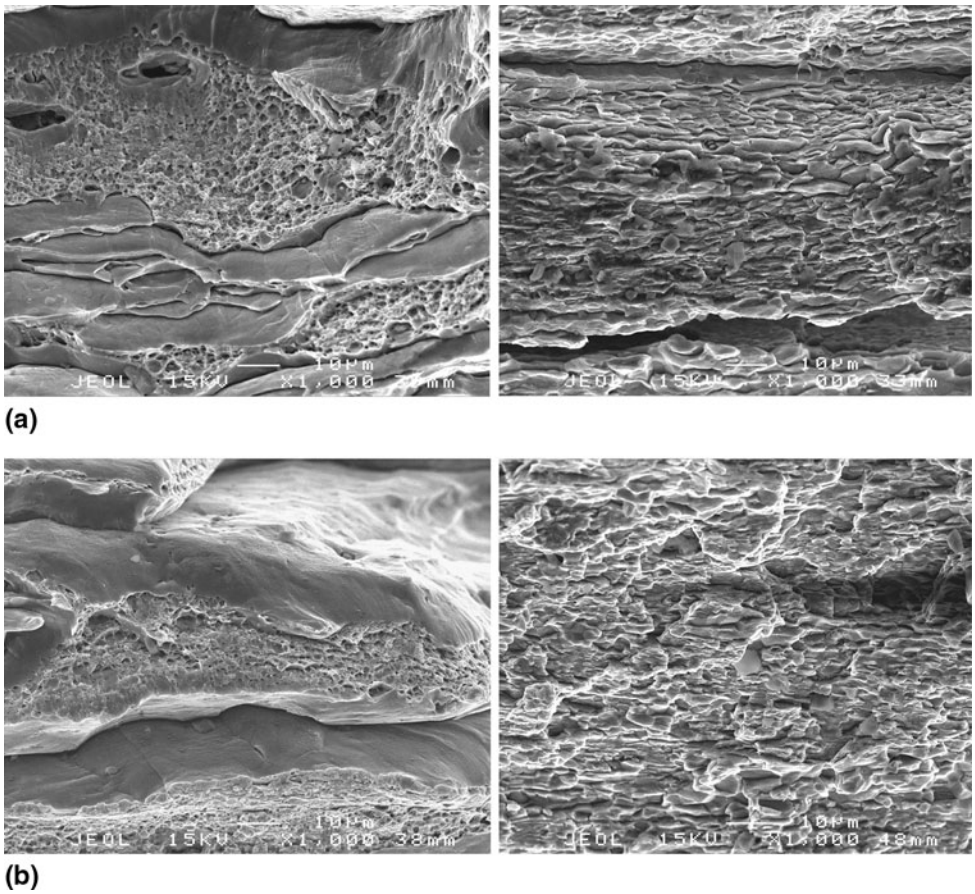


**Fig. 32** (a) SEM micrograph at 1000× magnification. As received. (b) SEM micrograph of 1000× magnification. 200 °C for 40 min process 1. (Left) Al 2099; (Right) 2195

**Table 8 Percent elongation tables for both 2099 and 2195, process 1**

| Percent elongation process 1 (Al 2195\|Al 2099) | | | | | | | | |
|---|---|---|---|---|---|---|---|---|
| | 200 °C | | 220 °C | | 240 °C | | 250 °C | |
| Time, min | Non-salt spray | Salt spray | Non-salt spray | Salt spray | Non-salt spray | Salt spray | Non-salt spray | Salt spray |
| 5 | 7.2\|16.0 | 2.9\|10.2 | 6.6\|10.4 | 4.5\|9.9 | 9.6\|11.4 | 3.8\|9.3 | 7.2\|11.2 | 3.4\|9.3 |
| 10 | 7\|8.7 | 4\|8.8 | 6.6\|10.0 | 6.4\|8.8 | 9.1\|12.0 | 5\|10.0 | 6.9\|9.8 | 3.3\|10.8 |
| 20 | 7.1\|10.0 | 2.9\|7.5 | 8.2\|13.0 | 4.5\|9.6 | 8.1\|10.3 | 4.5\|10.0 | 6.7\|8.8 | 4.3\|8.0 |
| 40 | 7.1\|9.5 | 2.8\|10.9 | 4.6\|9.6 | 5.5\|9.2 | 6.4\|10.2 | 4.1\|9.5 | 7.2\|10.8 | 4.6\|8.8 |
| 60 | 10.5\|10.3 | 2\|9.6 | 6.9\|10.7 | 3.6\|8.6 | 7.9\|11.2 | 5.3\|10.1 | 8\|10.1 | 5.8\|9.7 |

**Table 9 Percent elongation tables for both 2099 and 2195, process 2**

| Percent elongation process 2 (Al 2195\|Al 2099) | | | | | | | | |
|---|---|---|---|---|---|---|---|---|
| | 200 °C | | 220 °C | | 240 °C | | 250 °C | |
| Time, min | Non-salt spray | Salt spray | Non-salt spray | Salt spray | Non-salt spray | Salt spray | Non-salt spray | Salt spray |
| 5 | 6.45\|11.2 | 4.3\|9.8 | 8.2\|11.2 | 5\|9.1 | 9\|N/A(a) | 4.2\|11.0 | 11\|11.4 | 3.6\|10.0 |
| 10 | 6.5\|9.6 | 5.3\|9.7 | 8.2\|11.2 | 4.4\|9.3 | 7.2\|N/A(a) | 5.8\|10.6 | 6.3\|9.8 | 5.1\|9.7 |
| 20 | 6.5\|7.5 | 3.8\|9.4 | 9.3\|11 | 4.7\|9.4 | 5.5\|N/A(a) | 4.5\|9.6 | 8.5\|10.0 | 4.9\|8.5 |
| 40 | 7.8\|8.1 | 5.7\|9.8 | 8.2\|11.3 | 4.4\|9.8 | 6.9\|N/A(a) | 4.4\|10.4 | 6.9\|9.1 | 5.4\|8.9 |
| 60 | 5.1\|8.8 | 4.7\|8.8 | 7\|11.2 | 3.8\|9.8 | 7.5 \|N/A(a) | 5.5\|10.0 | 7.9\|9.7 | 6.6\|10.2 |

(a) The percent elongation was not calculated for samples which broke outside the gage length. The position of the fracture was slightly away from the gage, and the samples never failed in the radius or in the grip

Although the strength values of the 2195 alloy are initially higher (Ref 24), the strength values, however, decline much faster than those of the 2099 alloy. Also the 2195 alloy exhibits a more brittle behavior especially after exposure to the salt bath environment. This is due maybe partially to its lower Zn content (Ref 20).

## 5. Summary

The best RRA processes for the 2195 alloy were at 200 °C for all times (5, 10, 20, 40, and 60 min). As retrogression time and temperature increased, the strength values decreased. The salt-sprayed samples had about the same strength values as the non-salt-sprayed samples. However, the percent elongation of the salt-sprayed samples were significantly lower than those that which were not sprayed. Both processes 1 and 2 appear to yield the same results.

The 2195 alloy had higher initial strength values as compared to those of the 2099 alloy, but these values dropped faster as the retrogression time and temperature increased. The percent elongation of the 2195 alloy significantly deteriorated with or without the salt spray test as compared to the 2099 alloy. The percent elongation of the 2099 alloy was consistently high even after exposure to the salt bath environment. Interestingly, the salt-sprayed 2099 samples exhibited consistently higher strength values as compared to the non-salt-sprayed samples. The microstructures of the fractured tensile bars were in accordance with the ductility data for both alloys.

## References


1. B. Cina, Reducing Stress Corrosion Cracking in Aluminum Alloys, U.S. Patent 3,856,584, 24 December 1974
2. R.S. Kaneko, RRA: Solution for Stress Corrosion Problems with T6 Temper Aluminum, *Met. Prog.*, 1980, **117**, p 41–43
3. M. Talianker and B. Cina, Retrogression and Reaging and the Role of Dislocations in the Stress Corrosion of 7000-Type Aluminum Alloys, *Metall. Trans. A*, 1989, **20A**, p 2087–2092
4. J.K. Park, Influences of Retrogression and Reaging Treatments on the Strength and Stress Corrosion Cracking Resistance of Aluminum Alloy 7075-T6, *Mater. Sci. Eng. A*, 1988, **103**, p 223–231
5. J.K. Park and A.J. Ardell, Microstructure of the Commercial 7075 Al Alloy in the T651 and T7 Tempers, *Metall. Trans. A*, 1983, **14A**, p 1957–1965
6. J.K. Park and A.J. Ardell, Effect of Retrogression and Reaging Treatments on the Microstructure of Al-7075-T651, *Metall. Trans. A*, 1984, **15A**, p 1531–1543
7. P. Fleck, D. Calleros, M. Madsen, T. Trinh, D. Hoang, E.W. Lee, J. Foyos, and O.S. Es-Said, Retrogression and Reaging of 7075 T6 Aluminum Alloy, *Aluminum Alloys, Their Physical and Mechanical Properties—Proceedings ICAA7*, Part 1(Charlottesville, VA), Trans Tech Publications, 2000, p 649–654
8. P. Fleck, K. Koziar, E. Fromer, P. Herbe, G. Davila, M. Lead, J. Foyos, E.W. Lee, and O.S. Es-Said, Retrogression and Reaging of 7249 Plates, *Light-Weight Alloys for Aerospace Applications*, K.V. Jata, Ed., TMS, Warrendale, PA, 2001, p 99–108
9. P. Fleck, K. Koziar, J. Davila, H. Pech, E. Fromer, M. Leal, J. Foyos, E.W. Lee, and D. Tenney, A Review of the Effect of Retrogression and Reaging on Aluminum Alloy 7249, *LiMat3*, Center for Advanced Aerospace Materials, Puhang University of Science, Pusan, Korea, 2001, p 559–564
10. J. Na, G. Xiang, and Z. Zi-Qioa, Microstructure Evolution of Aluminum Lithium Alloy 2195 Undergoing Commercial Production, *Trans. Nonferrous Met. Soc. China*, 2010, **20**, p 740–745

11. J.H. Sanders, Investigation of Grain Boundary Chemistry in Al-Li 2195 Welds using Auger Electron Spectroscopy [J], *Thin Solid Films*, 1996, **227**(1/2), p 121–127
12. M.C. Chatuvedi and D.L. Chen, Effect of Specimen Orientation and Welding on the Fracture and Fatigue Properties of 2195 Al-Li Alloy [J], *Mater. Sci. Eng. A*, 2004, **389**, p 465–469
13. M.L. Bairwa, S.G. Desai, and P.P. Date, Identification of Heat Treatments for Better Formability in an Aluminum Lithium Alloy Sheet, *J. Mater. Eng. Perform.*, 2005, **14**, p 623–633
14. M. Romios, R. Tiraschi, C. Parrish, H. Babel, J.R. Ogren, and O.S. Es-Said, Design of Multistep Aging Treatments of 2099 (C458) Al-Li Alloy, *J. Mater. Eng. Perform.*, 2005, **14**(5), p 641–646
15. "2195-T8R78 Al-Li Plates" Alcan Aerospace Brochure, April 2010, http://www.alcanaerospace.com
16. "ASTM B117" Ascott Analytical Equipment Limited and National Exposure Testing, April 2010, http://www.ascott-analytical.com/ASTMB117/
17. "ASTM E8" Instron Tension Testing of Metallic Materials, April 2010, http://www.instron.us/wa/home/default_en.aspx
18. O.S. Es-Said, W.E. Frazier, and E.W. Lee, The Effect of Retrogression and Re-Aging on the Properties of the 7249 Aluminum Alloys, *JOM*, 2003, p 45–48
19. N. Ward, A. Tran, A. Abad, E.W. Lee, M. Hahn, E. Fordan, and O.S. Es-Said, The Effects of Retrogression and Reagging on Aluminum Alloy 2099 (C458), *J. Mater. Eng. Perform.* (Accepted)
20. Registration Record Series, Teal Sheets, May 2010, http://www.aluminum.org
21. E.A. Starke, Jr. and C.P. Blankenship, Jr., Aluminum Lithium Alloys, *Aluminum-Lithium Alloys for Aerospace Applications*, Proceedings of a Workshop, NASA, George Marshall Space Flight Center, Alabama, May 17–19, 1994
22. C. Giummarra, B. Thomas, and R. Rioja, New Aluminum Lithium Alloys for Aerospace Applications, *Proceedings of the Light Metals Technology Conference*, 2007, http://www.alcoa.com
23. N. Aizpuru, D. Le, J. McDonald, L. McLennan, S. Tewfik, E.W. Lee, D. Piatkowski, J. Foyos, J. Ogren, and O.S. Es-Said, The Effects of Flash Annealing on the Mechanical and Electrical Properties of Previously used AM2 Mats Composed of AL 6061-T6, *Eng. Fail. Anal. J.*, 2005, **12**, p 691–698
24. F.S. Bovard, Advanced Aluminum Technologies, *NSRP—Product Design & Materials Technology Panel Meeting*, Collection of Power Point Presentation Slides, 14 Feb 2008, http://www.nsrp.org